Coordinated Sensing and Tracking for Mobile Camera Platforms

C. Ding, A. A. Morye, J. A. Farrell, A. K. Roy-Chowdhury
University of California, Riverside

***Abstract*—This work focuses on developing optimal routing and camera control strategies for multiple mobile PTZ camera platforms cooperatively tracking a stochastic target moving on the ground. The vehicles are modeled as planar Dubins vehicles traveling at a fixed speed and height. The target is tracked using an Extended Kalman Consensus Filter that estimates the target location on the ground plane and the associated error covariance. Using dynamic programming, we compute optimal coordinated control policies which minimize the expected fused geolocation error covariance. The output of this process leads to the trajectories of the vehicles and the PTZ settings of the cameras. We show results on both ground and air vehicles tracking a target whose dynamics is modeled by a stochastic difference equation and discuss the implications of the results. The main contribution of the work is in the development of an optimal strategy for simultaneous vehicle navigation and camera parameter selection to maximize the tracking performance of stochastic targets where the risk of losing the target needs to be considered.**

I. Introduction

In recent years, small unmanned vehicles, both terrestrial and aerial, have found application in tasks such as surveillance, search and rescue, mapping, and real-time monitoring. Determination of the world-frame coordinates of the tracked object is referred to as *geolocation*. The focus of this work is on the problem of optimally coordinating the motions of multiple vehicles, each equipped with pan-tilt-zoom (PTZ) cameras, for the purpose of tracking a target, with underlying stochastic dynamics, moving on the ground. It leads to the development of optimal routing and camera PTZ parameter control strategies that maximize the tracking performance (i.e., minimize the geolocation error). The combined optimization of routes and camera parameters, and the consideration of stochasticity in the target dynamics, sets this work apart from the research in both camera networks [1] and dynamic vehicle routing [2], as well as previous work on UAV coordination for optimal tracking [3].

The dynamics of each target is modeled using a stochastic difference equation. An Extended Kalman Filter [4] is used to track the target on the ground, using measurements obtained from video. Geolocation for video cameras is achieved by using the pixel coordinates, intrinsic and extrinsic camera parameters, and the terrain data to estimate the location and associated error covariance of the target in the world frame. Using dynamic programming, we compute optimal coordinated control policies, yielding the vehicle trajectories and camera PTZ settings, which minimize the expected fused geolocation error covariance. We show results for both ground and air vehicles, report the optimal trajectories, PTZ settings and the geolocation error covariance.

A. Related Work

There has been a significant amount of work in coordinated target tracking. For two vehicles, maintaining a 90° angle of separation in relation to the target minimizes the fused geolocation error covariance as the camera-to-target line-of-sight vectors are orthogonal [5]. Much work, such as in [6] and [7], has been dedicated to designing controllers with angular separation as the goal. Methods to achieve diverse viewing angles have also been explored in [8] and [9]. The controller developed in [7] tasks aerial vehicles to orbit the target periodically while maintaining a fixed standoff distance. Each of these studies design control laws that should produce better geolocation estimates without explicitly considering the geolocalization. More recently, [3] and [10] have directly optimized the geolocation error covariance using online receding horizon controllers.

The geolocation error is highly sensitive to the relative position of the vehicle to the target, and the zoom capabilities of the video sensor. When the relative horizontal distance between the vehicle and target, with respect to the height, is large, the resulting error covariance is significantly elongated in the viewing direction. As this relative horizontal distance shrinks, the geolocation error covariance tends towards circularity. This effect is shown in Fig. 1. Thus, purely from a camera-measurement-based state estimation perspective, the ideal path for the tracking vehicle would be to match the target's motin while directly overhead. However, the different dynamics of the tracking vehicles and the targets may preclude such positions from being maintained or even acquired. Additional vehicles working in concert may be able acquire measurements resulting in a fused geolocation error covariance of a circular nature.

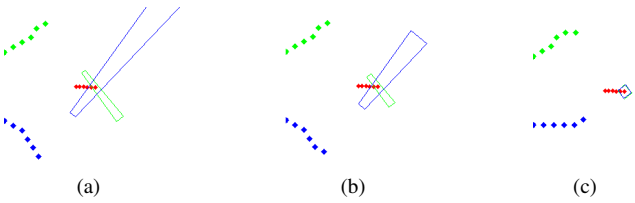

Fig. 1. Example fields of view (FOVs) from a height of a) 10m, b) 15m and c) 50m. The vehicles and the corresponding FOVs at the last position are in blue and green. The target is in red. The figure shows that the FOV becomes less elongated as height increases.

Our work differs significantly from the work above in two important ways. First, we consider the risk of failing to image a target. For non-deterministic targets, there is a very real risk of failing to image the target if a significant portion of its

TABLE I
NOTATION SUMMARY

Parameter	Variable
Pan, Tilt, Zoom (Focal Length)	(ρ, τ, F)
No. of Cameras Platforms, No. of planning steps	N_c, N_s
(ρ, τ, F) settings vehicle i	$\mathbf{a}_i$
State of all vehicles and target at time t_k	$\mathbf{z}(k)$
Expected value of measurements acquired in state $\mathbf{z}(k)$	$V(\mathbf{z}(k))$
Global Utility function	$U_0(\mathbf{z})$
Recursive Global Utility function	$U_k(\mathbf{z})$
Expected value of $U(\mathbf{a})$ over all targets	$V(\mathbf{a})$
State vector for the target	$\mathbf{x}$
State est., state est. covariance for the target	$\hat{\mathbf{x}}$, $\mathbf{P}$
Measurement information matrix, state est. information matrix	$\mathbf{J}$, $\mathbf{P}^{-1}$
Measurement vector, Measurement covariance	$\mathbf{u}$, $\mathbf{C}$
Rotation matrix from frame a to frame b	${}^b_a\mathbf{R}$
Linearized mapping from world to image frame	$\mathbf{H}$

probable locations is not covered by the FOV. Second, we consider PTZ cameras and optimize these settings *jointly* with the vehicle routes. This leads to a optimal joint control policy for a long horizon using dynamic programming by minimizing the expected fused geolocation error covariance. The benefit of this approach is that we can evaluate and plan long term paths for multiple UAVs tracking a non-deterministic target while minimizing the risk of losing track it.

The rest of the paper is organized as follows. In Section II we discuss target tracking using the Extended Kalman Filter, the video-based measurement model, the geolocation error covariance, and the dynamics of the mobile platform. The proposed dynamic programming approach, including both the cost function and PTZ computations, are described in Section III. Section IV contains a discussion on the simulation and the results. We conclude with Section V with a summary of the discoveries and the directions for future work on the topic.

II. TARGET AND VEHICLE MODELS

We consider mobile camera platforms (i.e., vehicles) tasked with tracking moving targets. Each of these vehicles moves at fixed forward speed while maintaining a constant altitude. The target is located on the ground plane and has a non-deterministic trajectory. A PTZ camera is mounted on each of the vehicles and is used to acquire measurements of the target. The main objective is to optimize the motion of the vehicles and PTZ settings of the cameras with respect to the joint estimation error covariance across all vehicles for each target. It is assumed that each vehicle can communicate with other nearby vehicles or a base station to fuse acquired measurements. It is also assumed that the world frame location of each vehicle and the extrinsic camera-to-vehicle parameters are accurately known. In this section, we first describe how the target vehicle dynamics are modeled and estimated using an Extended Kalman Filter. We then discuss the measurement model and the resulting relationship between the image plane observation and the geolocation error covariance. Finally, we present the discretized Dubins vehicle model for the camera platforms.

A. Target Model

For target tracking in the world frame we consider a dynamic model with a linearized discrete time state propagation:

$$\hat{\mathbf{x}}(k+1) = \mathbf{\Phi}\mathbf{x}(k) + \boldsymbol{\gamma}(k); \tag{1}$$

and, a nonlinear observation model for each camera:

$${}^i\mathbf{u}(k) = h_i(\mathbf{x}(k)) + {}^i\boldsymbol{\eta}(k), \text{ for } i = i, \ldots, N_c \tag{2}$$

where $\boldsymbol{\gamma}(k) \sim N(0, \mathbf{Q})$ and ${}^i\boldsymbol{\eta}(k) \sim N(0, \mathbf{C}_i)$. We define the state of the target at time t_k as $\mathbf{x}(k) = \left[{}^w\mathbf{p}, {}^w\mathbf{v}\right]^\top$ where ${}^w\mathbf{p}$ and ${}^w\mathbf{v}$ are the target vehicle's position and velocity vectors. The superscripts w and i are respectively used to denote the world and image frames of reference. Since we have a linear prediction model with a nonlinear measurement model for each vehicle we use the Extended Kalman Filter. The iterations of our EKF in information form are as follows.

- Correction

$$\begin{aligned} \mathbf{M}(k)^{-1} &= \mathbf{P}(k)^{-1} + \mathbf{H}_i(k)^\top \mathbf{C}_i(k)^{-1}\mathbf{H}_i(k) \\ \mathbf{K}(k) &= \mathbf{M}(k)\mathbf{H}_i(k)^\top \mathbf{C}_i(k)^{-1} \\ \mathbf{v}(k) &= {}^i\mathbf{u}(k) - h_i(\hat{\mathbf{x}}(k)) \\ \mathbf{x}(k) &= \hat{\mathbf{x}}(k) + \mathbf{K}(k)\mathbf{v}(k). \end{aligned} \tag{3}$$

- Prediction

$$\begin{aligned} \mathbf{P}(k+1) &= \mathbf{\Phi}(k)\mathbf{M}(k)\mathbf{\Phi}(k)^\top + \mathbf{Q}(k) \\ \hat{\mathbf{x}}(k+1) &= \mathbf{\Phi}(k)\mathbf{x}(k) \end{aligned} \tag{4}$$

The prior fused information matrix $\mathbf{J} = \mathbf{P}^{-1}$ can be represented in block form as

$$\mathbf{J} = \begin{bmatrix} \mathbf{J_{pp}} & \mathbf{J_{pv}} \\ \mathbf{J_{vp}} & \mathbf{J_{vv}} \end{bmatrix}, \tag{5}$$

where $\mathbf{J_{pp}}$ represents the position information matrix and $\mathbf{J_{vv}}$ represents the velocity information matrix.

B. Measurement Model

The video sensor mounted on each mobile platform acquires image plane measurements of all targets in its field of view (FOV). The two main coordinate frames that are used in video tracking are the world coordinate frames (also called the topographic frame), where the target and vehicle are located, and the sensor coordinate frame. This section presents the nonlinear and linearized measurement models. The linearization is performed relative to the estimated position ${}^w\hat{\mathbf{p}}$ of the target vehicle on the ground plane and closely follows the work presented in [11]. For the remainder of this section, all measurement vectors are computed at t_k with the time argument and subscripts dropped to simplify notation.

We assume that the topographic position of the i-th mobile camera ${}^w\hat{\mathbf{p}}^i$, and the estimated target position ${}^w\hat{\mathbf{p}}$ are known. The rotation matrix ${}^i_w\mathbf{R}(\rho_i, \tau_i)$ and focal length F_i are also assumed to be known functions of the pan, tilt and zoom settings of the gimballed video sensor.

Let the position of the target in the i-th camera frame be ${}^i\mathbf{p} = \left[{}^ix, {}^iy, {}^iz\right]^\top$. Using the standard pin-hole camera model

with perspective projection [12], the projection of ${}^i\mathbf{p}$ onto the image plane of camera i is ${}^i\mathbf{u} = \left[\begin{array}{ccc} F_i & \frac{{}^ix}{{}^iz}, & F_i & \frac{{}^iy}{{}^iz}, & F_i \end{array} \right]^\top$. Thus, the image plane measurement ${}^i\mathbf{u}$ is

$$ {}^i\mathbf{u} = \left[\begin{array}{c} F_i \ \frac{{}^ix}{{}^iz} \\ F_i \ \frac{{}^iy}{{}^iz} \end{array} \right] + {}^i\boldsymbol{\eta} \tag{6} $$

where the measurement noise ${}^i\boldsymbol{\eta} \sim \mathcal{N}(\mathbf{0}, \mathbf{C}_i)$ with $\mathbf{C}_i > \mathbf{0}$ and $\mathbf{C}_i \in \Re^{2\times 2}$.

Given the estimated state and camera model, the estimated target position in the i-th camera frame is ${}^i\hat{\mathbf{p}} = \left[{}^i\hat{x}, {}^i\hat{y}, {}^i\hat{z}\right]^\top$ and the predicted estimate of the measurement is

$$ {}^i\hat{\mathbf{u}} = \left[\begin{array}{c} F_i \ \frac{{}^i\hat{x}}{{}^i\hat{z}} \\ F_i \ \frac{{}^i\hat{y}}{{}^i\hat{z}} \end{array} \right]. \tag{7} $$

The measurement residual ${}^i\tilde{\mathbf{u}}$ is defined as

$$ {}^i\tilde{\mathbf{u}} = {}^i\mathbf{u} - {}^i\hat{\mathbf{u}}. \tag{8} $$

1) Observation Matrix $\boldsymbol{H}_i$: Given ${}^w\mathbf{p}_i$, ${}^w\hat{\mathbf{p}}$, and ${}^i_w\mathbf{R}$, subsequent analysis will use the linearized relationship given by the first order Taylor series expansion of eqn. (6) around the estimated state. The linear relationship between the measurement residual and the state error is

$$ {}^i\mathbf{u} - {}^i\hat{\mathbf{u}} \approx \ \mathbf{H}_i({}^w\mathbf{p} - {}^w\,\hat{\mathbf{p}}) \tag{9} $$

where $\mathbf{H}_i = \frac{\partial {}^i\mathbf{u}}{\partial {}^w\mathbf{p}}\Big|_{{}^w\hat{\mathbf{p}}} \in \Re^{2\times 3}$. Taking the partial derivatives as defined above, it is straightforward to show that

$$ \mathbf{H}_i \ = \ \frac{F_i}{({}^i\hat{z})^2} \left[\begin{array}{c} {}^w\mathbf{N}_1^\top \\ {}^w\mathbf{N}_2^\top \end{array} \right] \tag{10} $$

where ${}^w\mathbf{N}_1 = {}^w_i\mathbf{R}{}^i\mathbf{N}_1$ for ${}^i\mathbf{N}_1 = \left[{}^i\hat{z}, 0, -{}^i\hat{x}\right]^\top$, and ${}^w\mathbf{N}_2 = {}^w_i\mathbf{R}{}^i\mathbf{N}_2$ for ${}^i\mathbf{N}_2 = \left[0, {}^i\hat{z}, -{}^i\hat{y}\right]^\top$, are the vectors normal to the vector from camera i's origin to the target's estimated position ${}^i\hat{\mathbf{p}}$. Let us define matrix ${}^w\mathbf{N}^\top$ as follows:

$$ {}^w\mathbf{N}^\top = \left[\begin{array}{c} {}^w\mathbf{N}_1^\top \\ {}^w\mathbf{N}_2^\top \end{array} \right] \tag{11} $$

The observation matrix can then be written as

$$ \mathbf{H}_i = \frac{F_i}{({}^i\hat{z})^2} {}^w\mathbf{N}^\top. \tag{12} $$

Given the linearized mapping between the image and world frames, the quantity $\mathbf{J}_i = \mathbf{H}_i^\top \mathbf{C}_i^{-1} \mathbf{H}_i$ is the geolocation information matrix of the measurement conditioned on the target being in the FOV of i-th camera.

C. Camera Platform Model

A Dubins vehicle is a planar vehicle that has a fixed forward velocity with a bounded turning radius. This provides a simple model for a airborne mobile camera platforms with both a fixed altitude and velocity. The model neglects sideslip. For the i-th vehicle, let ${}^w\mathbf{p}_i = \left[{}^wx_i, {}^wy_i, {}^wz_i\right]^\top$ denote its position in the world frame, let $\mathbf{a}_i = [\rho_i, \tau_i, F_i]$ be the pan, tilt and focal length of the camera, and ψ_i denote its heading. The kinematics of the camera platform with fixed altitude ${}^wz_i$, velocity v_i and max turning rate $w_{max} > 0$, are described by

$$ \begin{aligned} {}^w\dot{x}_i(k) &= v_i cos(\psi_i(k)) \\ {}^w\dot{y}_i(k) &= v_i sin(\psi_i(k)) \\ \dot{\psi}_i(k) &= u_i(k), |u_i| \leq w_{max}. \end{aligned} \tag{13} $$

To discretize the Dubins vehicle dynamics, we apply a zero order hold (ZOH) on the control input at a sampling time of 1 second [3].The discrete-time equivalent model for non-zero input is

$$ \begin{aligned} {}^wx_i{}^+ &= \frac{v_i}{u_i}\left[sin(\psi_i + u_i) - sin(\psi_i)\right] + x_i \\ {}^wy_i{}^+ &= \frac{v_i}{u_i}\left[cos(\psi_i) - cos(\psi_i + u_i)\right] + y_i \\ \psi_i{}^+ &= u_i + \psi_i, \end{aligned} \tag{14} $$

and for zero input is

$$ \begin{aligned} {}^wx_i{}^+ &= v_i cos(\psi_i) + x_i \\ {}^wy_i{}^+ &= v_i sin(\psi_i) + y_i \\ \psi_i{}^+ &= \psi_i. \end{aligned} \tag{15} $$

Because Dubin vehicles use only three inputs (left, straight, right), $u_i(k) \in U$ where $U = \{-w_{i,max}, 0, w_{i,max}\}$.

III. Optimal Vehicle Routes and Camera Settings

The technique of dynamic programming can be used to solve a wide array of applications described by dynamic equations-of-motion that require optimized paths. We apply dynamic programming to produce an optimal control policy for a group of mobile cameras tracking a stochastic target. We present the utility function, followed by the computation of the PTZ settings. Naive implementation of dynamic programming results in an exponential time algorithm. By considering relative vehicle-to-target coordinates instead of absolute coordinates, we reduce the total amount of computation.

A. Utility Function

The utility function is designed to optimize estimation performance over a planning horizon. Performance is quantified as a function of the expected fused geolocation information

$$ E\left\langle \mathbf{J} \right\rangle = \sum_{i=1^{N_c}} \mathbf{J}_i Pr\{{}^w\mathbf{p} \in FOV_i\} \tag{16} $$

$$ = \sum_i \mathbf{J}_i \int_{FOV_i} p_{\mathbf{p}}(\boldsymbol{\zeta})\, d\boldsymbol{\zeta}. \tag{17} $$

The dummy variable $\boldsymbol{\zeta}$ is integrated over the ground plane and $p_{\mathbf{p}}$ is the Normal distribution $\mathcal{N}({}^w\hat{\mathbf{p}}, \mathbf{P}^-_{\mathbf{pp}})$ of the predicted position of the target in the global frame at time t_k.

For optimization, we choose a function $g\left(E\left\langle \mathbf{J} \right\rangle\right) : \mathbf{S}^n_{++} \mapsto \Re^+$. Ideally, g is a convex function. For this paper, we choose g to be the trace. The trace is easily computed and linear, but has the deficiency that it can be increased by increasing one diagonal element while leaving another component near zero, yielding an elongated estimation error ellipsoid.

Algorithm 1 $U_k(\mathbf{z})$

for each the i-th camera platform **do**
  Compute $\mathbf{a}_i = [\rho_i, \tau_i, F_i]$.
    First $[\rho_i, \tau_i]$ are obtained by centering the view on ${}^w\hat{\mathbf{p}}(k)$.
    Then map $\mathbf{P_{pp}}(k)$ to the image plane and compute F_i of the minimum bounding view.
end for
Propagate ${}^w\hat{\mathbf{x}}(k)$ and $\mathbf{P_{pp}}(k)$ to ${}^w\hat{\mathbf{x}}(k+1)$ and $\mathbf{P_{pp}}(k+1)$
for each $\mathbf{u} \in U^{N_c}$ **do**
  Compute $U_{k+1}(\mathbf{z})$ and save if max
end for
return V(**z**(k)) + max $U_{k+1}(\mathbf{z})$

The value function is

$$V(\mathbf{z}(k)) = trace(E\langle \mathbf{J_{pp}} \rangle), \tag{18}$$

where $\mathbf{z}(k)$ is concatenate vector of target camera platform state vectors. The resulting utility function is evaluated over a planning horizon of N_s time steps according to

$$U_0(\mathbf{z}) = \frac{1}{N_s} \sum_{k=0}^{N_s-1} V(\mathbf{z}(k)). \tag{19}$$

Backwards induction is used in dynamic programming to find the optimal control policy $\prod_k(\mathbf{z})$, which maps each state $\mathbf{z}(k)$ to an optimal control input for each vehicle at time t_k. Let N_c be the number of camera platforms. The optimal value is determined through the standard technique of value iteration where the optimal utility for Eqn. (19) is computed using the recursive function

$$U_k(\mathbf{z}) = \max_{\mathbf{u} \in U^{N_c}} (V(\mathbf{z}(k)) + U_{k+1}(f(\mathbf{z}, \mathbf{u}))), \forall \mathbf{z}, \tag{20}$$

from $k = N_s - 1$ to 0 with $V_{N_s}(\mathbf{z}) = 0, \forall \mathbf{z}$. The input $\mathbf{u}$ corresponding to the maximum value in Eqn. (20) is stored in $\prod_k(\mathbf{z})$. The state propagation model $f(\mathbf{z}, \mathbf{u})$ returns the state $\mathbf{z}(k+1)$.

The optimal PTZ settings $\mathbf{a}_i(k+1)$ of the video cameras are dependent on the expected state of the target $\hat{\mathbf{x}}(k+1)$ and the corresponding covariance $\mathbf{P}(k+1)$. The risk of failing to acquire an image of the target, is enhanced by ensuring that the expected position of the target and its associated error covariance ellipse are within the FOV of the camera. The amount of information obtained when imaging a target is directly proportional to the zoom of the camera. To reduce computation, instead of searching over the PTZ parameters during the optimization phase, we solve for the minimum bounding FOV of the target's uncertainty ellipse. The steps involved in this process are shown in Algorithm 1.

IV. Simulation

To demonstrate the effectiveness of our approach we prepared a simulation framework consisting of a $500m$ x $500m$ area. In this area we considered two vehicles with the objective of tracking a non-deterministic target. The target was initialized with a starting velocity of 5m/s along the x-axis and was propagated through time according to Eqn. (1). The parameters used for this dynamical model are as follows:

$$\mathbf{\Phi} = \begin{bmatrix} 1 & 0 & 1 & 0 \\ 0 & 1 & 0 & 1 \\ 0 & 0 & 1 & 0 \\ 0 & 0 & 0 & 1 \end{bmatrix}, \quad \mathbf{Q} = \begin{bmatrix} 33 & 0 & 50 & 0 \\ 0 & 33 & 0 & 50 \\ 50 & 0 & 100 & 0 \\ 0 & 50 & 0 & 100 \end{bmatrix}.$$

The target track was propagated for 120 seconds. We considered two scenarios: one for land-based camera platforms, and the other for aerial platforms. For the scenario considering land vehicles we set the altitude of the camera ${}^w z_i = 2m$ and for the scenario with aerial vehicles, ${}^w z_i = 100m$. In both cases the vehicles were initialized with a velocity $v_i = 15m/s$ along the x-axis. Planning for N_s seconds ahead is done at every time instant by propagating the estimated target state, and estimated error covariance from $\hat{\mathbf{x}}(k)$ and $\hat{\mathbf{P}}(k)$ through to $\hat{\mathbf{x}}(k+N_s)$ and $\hat{\mathbf{P}}(k+N_s)$. Planning for very long horizons is undesirable since the error in the expected location of a non-deterministic target increases as the target is propagated through time.

A. Terrestrial Vehicle

We first examine the target state estimation over a 120 second time window by two land based or low flying camera platforms.

The results for two land vehicles without planning ($N_s = 1$) are shown in Fig. 2. Fig. 2(a) shows the final paths taken by the two land vehicles. The nonexistent planning horizon means that each vehicle can and will take the best move available to it even if it results in a terrible set of choices at the next time step. This can also be seen at $t = 50$ where the geolocation error covariance is reduced by moving closer to the target at the expense of maintaining orthogonal error covariance ellipses. Because the video sensor is located only 2m above the ground, the resulting geolocation error covariance for a single measurement will be far from circular. In order to maintain an accurate target geolocation estimate, a second measurement is required, preferably with an orthogonal geolocation error covariance. This can be clearly seen in Fig. 2(d) and 2(e) for $t > 50$, where the covariance is significantly increased when the angle between the two vehicles, relative to the target, strays away from 90°.

Preplanning the trajectories for the entire 120 second duration is not only unreasonable for a stochastic target, it is also prohibitive in terms of computation. However, no planning, as we have just shown, can lead to situations causing large fluctuations in tracking accuracy. In the worst case the target track may be lost as the actual and expected vehicle positions diverge and actual position fails to be in the camera FOVs. The number of steps to plan ahead is dependent on the desired tracking accuracy and the amount of randomness in the vehicle motions, which is quantified by the process noise covariance matrix $\mathbf{Q}$. Fig. 3 shows the results of planning $N_s = 3$ steps ahead, for the same target trajectory. The computational cost of such a plan length is minimal and may be easily computed every second. From the trajectories exhibited in Fig. 3(a),

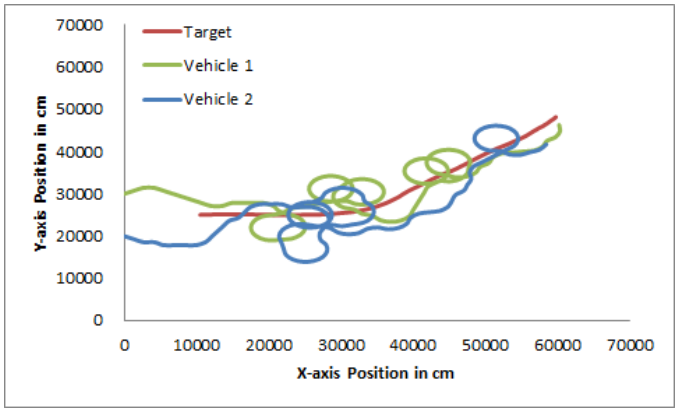

(a)

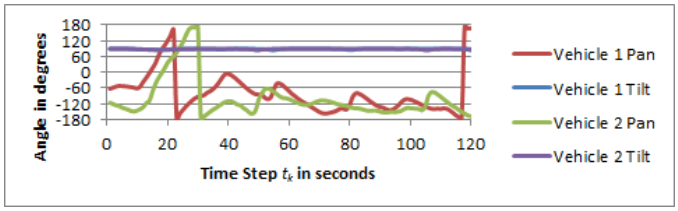

(b)

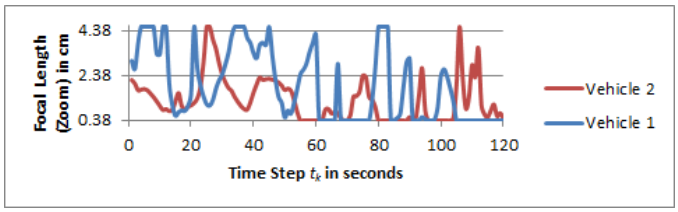

(c)

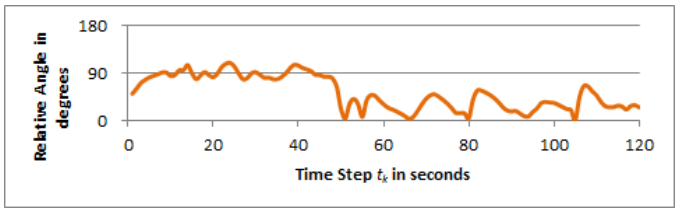

(d)

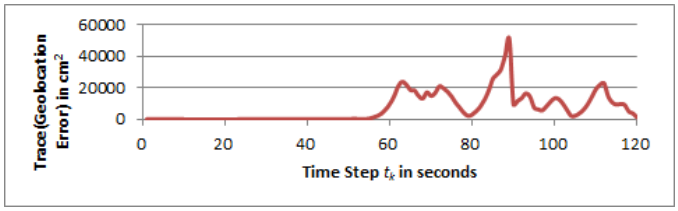

(e)

Fig. 2. Trajectories and results for 2 ground vehicles tracking a target with $N_s = 1$ planning steps. The explosion in tracking error from lack of planning can be demonstrated in Fig. 2(e).

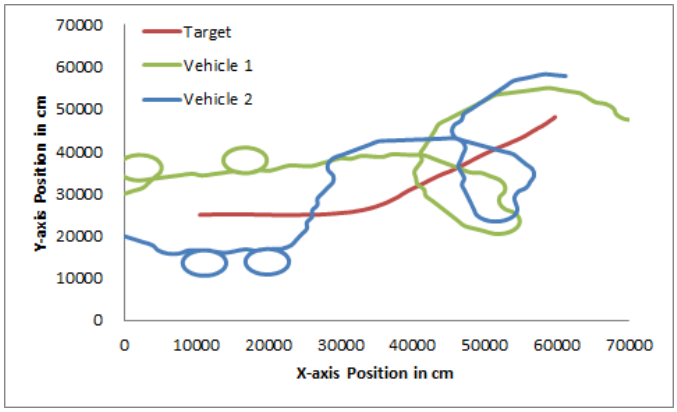

(a)

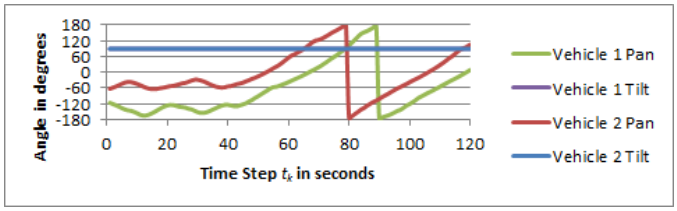

(b)

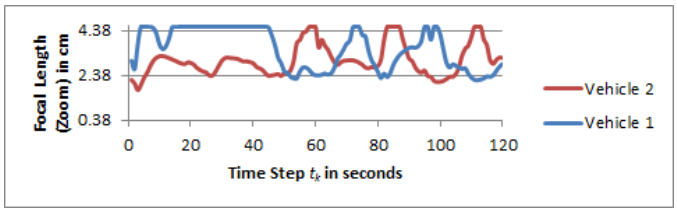

(c)

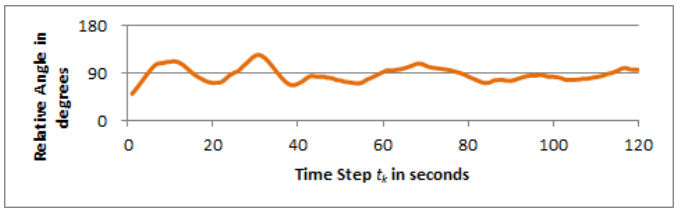

(d)

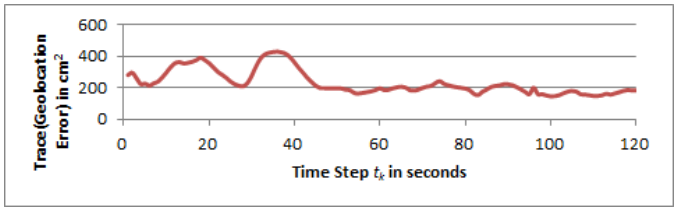

(e)

Fig. 3. Trajectories and results for 2 ground vehicles tracking a target with $N_s = 3$ planning steps. Maintenance of the optimal angular separation and the resulting smooth error covariance is displayed.

we can observe that the vehicles maintain a much further distance from the target than in the previous case. The relative angles between the two vehicles, shown in Fig. 3(d), also stay close to the 90° separation required for minimal instantaneous geolocation error covariance. The propagation of the expected target position and error covariance for the duration of the plan results in paths that ensure optimal measurements of targets that are governed by our model. It is also clear from Fig. 3(e) that the geolocation error covariance of the tracker is very smooth and not subject to the large fluctuations of the

previous scenario.

B. Aerial Vehicle

We now examine the target state estimation over a 120 second time window by two aerial camera platforms. Since the video sensor is located at a height of 100m, the resulting geolocation error covariance will tend more toward circularity than it did for the terrestrial vehicle. While a second measurement, with an orthogonal geolocation error covariance, is preferred, it is no longer necessary to maintaining good target geolocation estimates.

The paths traversed by the aerial vehicles are displayed in Fig. 4(a). It is immediately apparent that the vehicles have paths that follow the target more tightly that the planning scenario for ground vehicles. This enhances tracking performance as also be observed in the covariance plot of Fig. 4(e). Note that the angular separation of 90° is less critical as shown in 4(d).

V. Conclusion and Future Work

We have examined the defined and analyzed the path planning process for a stochastic target and multiple ground or aerial vehicles. Our results have confirmed that a 90° separation between the tracking vehicles is indeed preferable, especially for gorund vehicles. We have also shown the ability to maintain track of a stochastic target and the positive benefits that planning has on the tracking error covariance. Also, we have observed is that it is much easier for high flying aerial vehicles to track targets on a ground plane than it is for land based vehicles. Future work will consider multiple targets with multiple vehicles, distributed optimization, incorporation of smoothness constraints for the PTZ parameters, and incorporating vehicle uncertainty into the model.

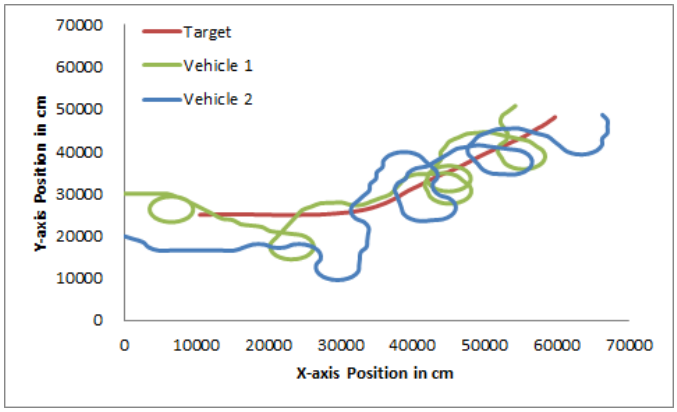

(a)

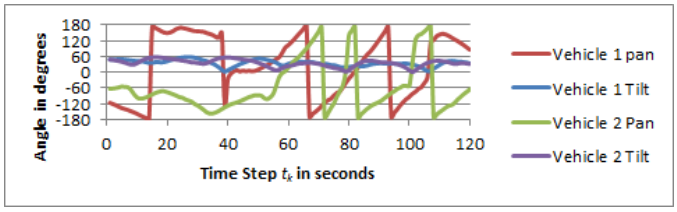

(b)

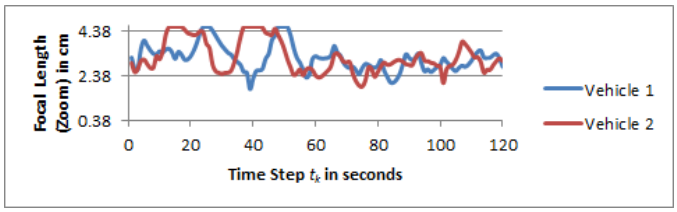

(c)

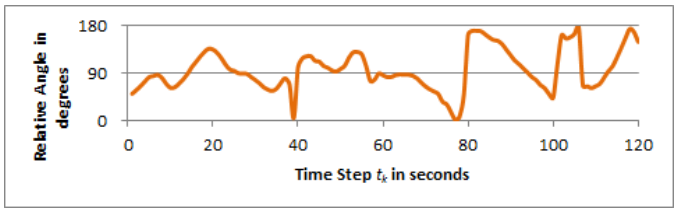

(d)

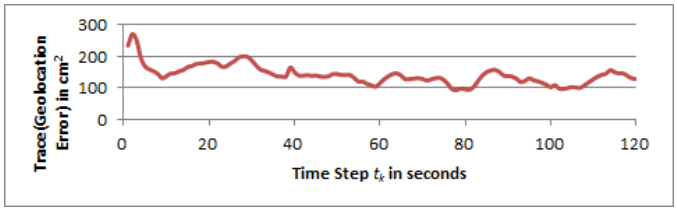

(e)

Fig. 4. Trajectories and results for 2 aerial vehicles tracking a target with $N_s = 3$ planning steps. A smooth covariance is achieved without requiring a consistent 90° angular separation.

References

[1] B. Song, C. Ding, A. Kamal, J. Farrell, and A. Roy-chowdhury, "Distributed camera networks," *Signal Processing Magazine, IEEE*, vol. 28, no. 3, pp. 20 –31, may 2011.

[2] F. Bullo, E. Frazzoli, M. Pavone, K. Savla, and S. Smith, "Dynamic vehicle routing for robotic systems," *Proceedings of the IEEE*, vol. 99, no. 9, pp. 1482–1504, 2011.

[3] S. Quintero, F. Papi, D. Klein, L. Chisci, and J. Hespanha, "Optimal UAV coordination for target tracking using dynamic programming," in *Proc. of the 49th Conf. on Decision and Contr.*, Dec. 2010.

[4] J.A. Farrell, "Aided Navigation: GPS with High Rate Sensors," pp. 72–75, 2008.

[5] G. Gu, R. Chandler, C. Schumacher, A. Sparks, and M. Pachter, "Optimum cooperative UAV sensing based on Cramer-Rao bound," in *American Control Conference*, June 2005.

[6] E. W. Frew, "Sensitivity of cooperative geolocalization to orbit coordination," in *AIAA Guidance, Navigation, and Control Conference*, Hilton Head, SC, Aug. 2007.

[7] D. B. Kingston, "Decentralized control of multiple uavs for perimeter and target surveillance," Ph.D. dissertation, Brigham Young University, Provo, Utah, Dec 2007.

[8] E. Lalish, *Oscillatory control for constant-speed unicycle-type vehicles*. University of Washington, 2007.

[9] D. Klein and K. Morgansen, "Controlled collective motion for trajectory tracking," in *American Control Conference*, 2006.

[10] M. Stachura, A. Carfang, and E. W. Frew, *Cooperative Target Tracking with a Communication Limited Active Sensor Network*, 2009.

[11] A. Morye, C. Ding, B. Song, A. Roy-Chowdhury, and J. Farrell, "Optimized Imaging and Target Tracking within a Distributed Camera Network," in *American Control Conference*, 2011.

[12] E. Trucco and A. Verri, *Introductory techniques for 3-D computer vision*. Prentice Hall, 1998.